REAL TIME DIABETIC FOOT ULCER DETECTION ON MOBILE PLATFORMS VIA DEEP LEARNING

Dr. N. Rajkumar
Professor(B.E., M.E., Ph.D)
Department of CSE
Vel Tech University(of Aff.)
Chennai, India
nrajkumar@veltech.edu.in

Suja Sangtam
B.Tech CSE(of Aff.)
Vel Tech University(of Aff.)
Chennai, India
vtu19312@veltech.edu.in

Nishant Raj Sharma
B.Tech CSE(of Aff.)
Vel Tech University(of Aff.)
Chennai, India
vtu19576@veltech.edu.in

Abstract*—Diabetic foot ulcers (DFU) are a common and serious complication in individuals with diabetes, and early detection plays a crucial role in effective treatment and prevention of further complications. Automated DFU Detection and Classification using Deep learning (DL) refers to the application of deep learning techniques to automatically detect and classify diabetic foot ulcers from medical images. DL, a subfield of machine learning, has shown promising results in medical imaging analysis, including diabetic foot ulcer detection. The use of deep learning in DFU detection provides various benefits, including the ability to learn complex features, adaptability to different image modalities, and the potential for high accuracy in detection and classification tasks. Therefore, this article introduces a novel sparrow search optimization (SSO) with deep learning enabled diabetic foot ulcer detection and classification (SSODLDFUDC) technique. The presented SSODL-DFUDC technique's goal lies in identifying and classifying DFU. The proposed technique employs the Inception-ResNet-v2 model for feature vector generation to accomplish this. Since the trial and error manual hyperparameter tuning of the Inception-ResNet-v2 model is a tedious and erroneous process, the SSO algorithm can be used for the optimal hyperparameter selection of the Inception-ResNet-v2 model which in turn enhances the overall DFU classification results. Moreover, the classification of DFU takes place using the stacked sparse autoencoder (SSAE) model. The comprehensive experimental outcomes demonstrate the improved performance of the SSODL-DFUDC system related to existing DL techniques.

***Index Terms*—Medical image analysis, deep learning, diabetic foot ulcer, sparrow search optimization, computer-aided diagnosis.**

I. Introduction

Amputation of the limb or foot may be caused by a diabetic foot ulcer (DFU) infection. The probability of survival can be lesser for patients having amputated limbs. It damages the livelihood of quality and distresses social participation and the outcome of these causes and tissue death because of diseases. The DFU is increasing rapidly. Because of the scarcity of specialists and lack of resources in the medication for diabetic foot ulcers, over a million diabetic patients at higher risk of diabetic Mellitus will lose out foot (partly) every year. Notably, for every 20 seconds, one diabetic foot functioned. A complete study of medical data was essential for specialists to accomplish a precise outcome. Conventional diagnostic techniques were labour-intensive and vulnerable to human errors. The computer-based diagnostic process's utility includes minimal performance enhancement. Current advancements in n wearable and mobile health gadgets help in controlling diabetes and its limitations, improving the standards of life and extending remission for patients by s controlling harmful sensing and foot pressure and inflammation. The development of novel-generation medical sensors recommends expanding such devices' utility in the medical field. In the contemporary healthcare mechanism, medical images are used for diagnosing several patient difficulties. Conventional approaches for analysis of DFU use hand-crafted rendered technique. However, research activities in the publication have displayed that learned attributes by deep neural networks (DNN) have high potential compared to classical hand-crafted features. Wide research was conducted to enhance the outcome of computerized are very popular in this sector since they were superior to other techniques. The common method that is utilized in the DL technique in medical image classification is convolutional neural networks (CNNs). The CNNs can efficiently derive valuable attributes for image segmentation, image classification, other vision tasks, and object detection. With the obtainability of large-scale trained data and high-performing modern application specific integrated circuit (ASICs) and graphics processing units (GPUs) and techniques related to CNNs have enhanced the precision of image classification. Renowned CNNs for general image classifier tasks involve ResNet, AlexNet, EfficientNet, and VGG. Such networks generally serve as the pillar of medical image classifier networks or directly enforce medical image classifications by transfer learning (TL) with pre-trained variables on large-scale datasets (e.g., ImageNet). Practically, labelling and collecting medical images were costly. TL was a potential way to overcome the need for medicinal trained data.

Identify applicable funding agency here. If none, delete this.

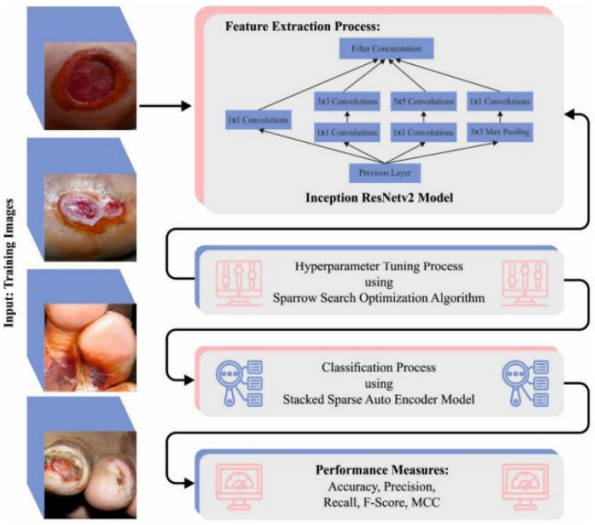

Fig. 1. Workflow

II. THE PROPOSED MODEL

A. FEATURE EXTRACTION USING OPTIMAL DL MODEL

The presented SSODL-DFUDC technique employed the Inception-ResNet-v2 model for feature vector generation. CNN is the algorithm of the DL algorithm. CNN is a progression of MLP developed for processing the dataset in grid form. CNN is exploited on the image dataset. The objective of the training model is to train the ANN module to reduce the error of predictive results of the model with the original dataset. The convolutional layer is a convolutional operation betwixt 2 vectors. In Eq. (1), it is convolutional of two functions where g(x) is named the convolutional kernel (filter) that is functioned in shifts on the vector F(x).

$$h(x) = F(x)g(x) = ZF(a)g(xa)eq \quad (1)$$

CNN comprises two phases. Initially, group images with feedforward. Then, use the backpropagation algorithm. Currently, the wrapping and cropping systems are performed to emphasize the categorised object before doing the classification. Next, training can be done by backpropagation and feed-forward techniques. The structure of CNN is split into two most important parts, such as the Fully-Connected Layer and Feature Extraction Layer. Inception-ResNetV2 is a CNN architecture trained originally on the ImageNet datasets, comprising 164 layers. The model has learned feature representation and is stronger for a large number of image types. This model accepts the input of 299 × 299 and the hybridization of two currently established networks, the modern architectural version, and residual links. There are sequences of filters, namely 1 × 1, 3 × 3, 5 × 5, and so on, merged with all the branch concatenation. The splittransformation-mixing architecture of the initiation model is perceived in its thick layer as a stronger representation. The residual connection enables the training of progressively DNN, leading to remarkable performance. In this work, the SSODL-DFUDC technique utilizes the SSO algorithm for hyperparameter tuning. The SSO is a recent heuristic approach inspired by the behaviours of sparrows foraging and avoiding predators and characteristics of group socialization. The SSO benefits from strong optimization ability, simple architecture, easier implementation, few control parameters, and so on. The SSO to converge to the present optimum solution is to jump towards the existing ideal solution's locality directly. Hence the SSO technique is better than the particle swarm optimization, grey wolf optimization, and gravity search algorithms with respect to robustness, accuracy, convergence speed, and stability. In this work, sparrows are

Fig. 2. Sample images a) Normal (Healthy) b) Abnormal (Ulcer)

alienated into vigilant and discoverer followers. The location of every sparrow corresponds to the solution. The position of each sparrow in the sparrow groups is characterized as X matrix:

$$\begin{matrix} X1,2 & \ldots & a1,d \\ \ldots & \ldots & \ldots \\ f([xm,1 & \ldots & xm,d]) \end{matrix}$$

h indicates the count of sparrows, and d denotes the dimension of the variable that is enhanced.where f ([xi,1, · · · , xi,d]) signifies the fitness value of i th sparrows.where t signifies the existing amount of iterations, and N signifies the maximum amount. indicates a random integer, and (0, 1]. R2 characterizes the alarm value that is an arbitrary integer, and R2 [0, 1][0, 1].ST signifies the safety threshold and ST [O.5, 1.0].Q shows the random number subjected to the standard distribution, and L represents the row vector whose element is equivalent to 1.

B. DFU CLASSIFICATION USING THE SSAE MODEL

In this study, the classification of DFU takes place using the SSAE model. Hinton, in 2006, proposed an Autoencoder (AE) paradigm of ANN, and it is extensively used in reduction dimensionality [33]. The primary objective is to train the model with a similar input and output dataset. The architecture

Class	Accuracy$_{bal}$	Precision	Recall	F-Score	AUC Score	MCC
Fold - 1						
Abnormal	99.02	99.27	99.02	99.15	99.17	98.34
Normal	99.31	99.08	99.31	99.19	99.17	98.34
Average	**99.17**	**99.17**	**99.17**	**99.17**	**99.17**	**98.34**
Fold - 2						
Abnormal	98.78	99.26	98.78	99.02	99.04	98.10
Normal	99.31	98.85	99.31	99.08	99.04	98.10
Average	**99.04**	**99.06**	**99.04**	**99.05**	**99.04**	**98.10**
Fold - 3						
Abnormal	98.78	99.26	98.78	99.02	99.04	98.10
Normal	99.31	98.85	99.31	99.08	99.04	98.10
Average	**99.04**	**99.06**	**99.04**	**99.05**	**99.04**	**98.10**
Fold - 4						
Abnormal	99.02	99.27	99.02	99.15	99.17	98.34
Normal	99.31	99.08	99.31	99.19	99.17	98.34
Average	**99.17**	**99.17**	**99.17**	**99.17**	**99.17**	**98.34**
Fold - 5						
Abnormal	99.02	99.27	99.02	99.15	99.17	98.34
Normal	99.31	99.08	99.31	99.19	99.17	98.34
Average	**99.17**	**99.17**	**99.17**	**99.17**	**99.17**	**98.34**
Fold - 6						
Abnormal	99.02	99.27	99.02	99.15	99.17	98.34
Normal	99.31	99.08	99.31	99.19	99.17	98.34
Average	**99.17**	**99.17**	**99.17**	**99.17**	**99.17**	**98.34**
Fold - 7						
Abnormal	98.78	99.26	98.78	99.02	99.04	98.10
Normal	99.31	98.85	99.31	99.08	99.04	98.10
Average	**99.04**	**99.06**	**99.04**	**99.05**	**99.04**	**98.10**
Fold - 8						
Abnormal	99.27	99.27	99.27	99.27	99.29	98.58
Normal	99.31	99.31	99.31	99.31	99.29	98.58
Average	**99.29**	**99.29**	**99.29**	**99.29**	**99.29**	**98.58**
Fold - 9						
Abnormal	99.02	99.27	99.02	99.15	99.17	98.34
Normal	99.31	99.08	99.31	99.19	99.17	98.34
Average	**99.17**	**99.17**	**99.17**	**99.17**	**99.17**	**98.34**
Fold - 10						
Abnormal	98.78	96.20	98.78	97.47	97.55	95.06
Normal	96.31	98.82	96.31	97.55	97.55	95.06
Average	**97.55**	**97.51**	**97.55**	**97.51**	**97.55**	**95.06**

Fig. 3. Classifier outcome of SSODL-DFUDC approach with distinct measures and folds.

of the AE network contains a hidden layer (HL) with m neurons, an input layer with n neurons, and an output layer with n neurons. Firstly, the n-dimension sample is mapped from the input to the hidden layers that characterize an encoding method of

$$h_{w_1,b_1}(x) R^{m} .eq \quad (2)$$

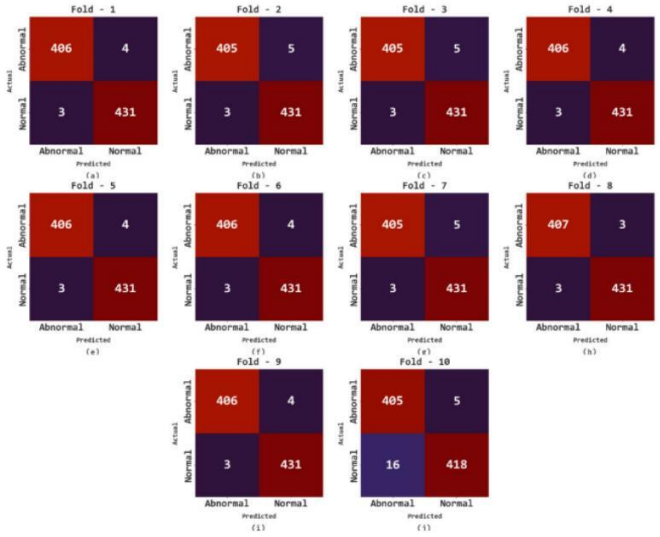

Fig. 4. Confusion matrices of SSODL-DFUDC approach (a-j) Fold 1-10

Following, hw1,b1(x) is decoded from the HL and mapped back to the n-dimensional space R n to recreate the input. The training process of the AE network is to perform the back propagation of error and continuously upgrade the network

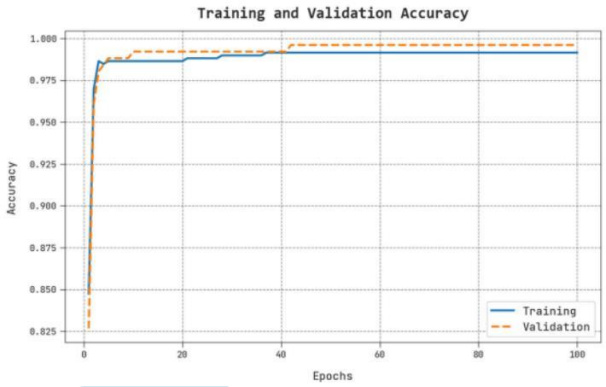

Fig. 5. TACC and VACC analysis of the SSODL-DFUDC system.

parameter for making the x˜ output to the x input, where x˜ = hw,b(x). Once the amount of HL nodes is larger, a sparse autoencoder (SAE) is adopted. To avoid overfitting, SAE added sparsity limitation to the AE network and exploited the sigmoid function as an activation function that inhibits the neuron in the hidden layer. The suppressed state implies that the neuron output is closer to zero. To guarantee that the neuron is suppressed, we must make the average activation degree closer to the sparse variable ρ, which is generally closer to zero.A penalty factor is added to the loss function of AE to accomplish the sparsity. j indicates the average activation degree of each neuron with every training sample, p denotes the sparse variable to be set. KL($\rho \parallel \rho$ entropy between ρ and ρj , viz., the KL divergence that value increases monotonically as the difference between ρ and ρj represents the relative .β denotes the weight of KL divergence. Once ρ and ρ ˆj are equivalent, then KL($\rho \parallel \rho$j) is equivalent to for getting its minimal value. Since ρ is generally closer to zero, p of each neuron in the HL would be controlled to be within a smaller range afterwards training, and the sparse representation of the input signal is lastly attained. The SSAE is encompassed by a single-layer SAE network, with the output of SAE of the preceding layer, which acts as an input of SAE of the following adjacent layer. By training the SAE network layer-wise, the SSAE network could eventually extract the feature concealed in the input for realizing reduction dimensionality.

III. EXPERIMENTAL VALIDATION

In this section, the DFU results of the SSODL-DFUDC technique are tested using a dataset from the Kaggle repository. The dataset includes 844 samples, with 410 abnormal and 434 standard samples, as demonstrated showcases the sample images of normal and abnormal. It represents the overall DFU detection results of the SSODL-DFUDC technique under different folds. The results showed that the SSODL-DFUDC technique has enhanced results under all folds. For instance, with fold1, the SSODL-DFUDC technique reaches average accubal, precn, and recal of 99.17% 99.17%, and 99.17%, respectively. Meanwhile, with fold-5, the SSODL-DFUDC system gains average accubal, precn, and recal of 99.17%,

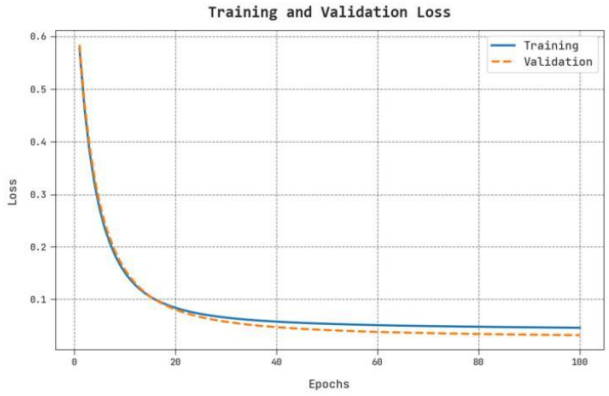

Fig. 6. TLS and VLS anlysis of SSODL-DFUDC system.

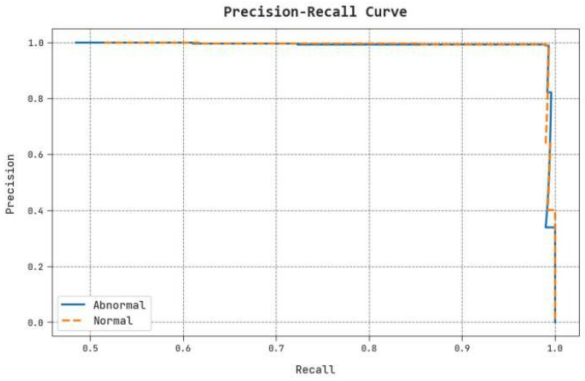

Fig. 7. Precision-recall analysis of SSODL-DFUDC system.

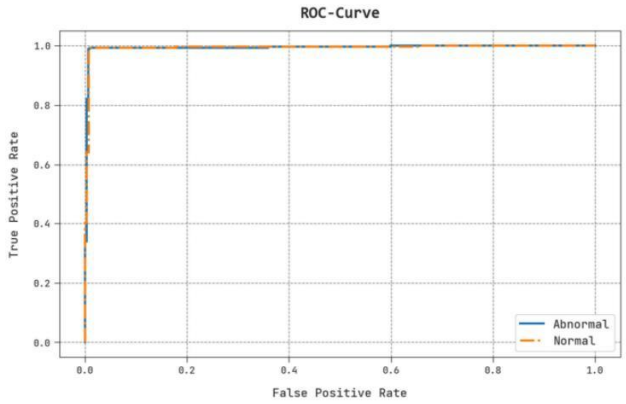

Fig. 8. ROC analysis of the SSODL-DFUDC system

99.17%, and 99.17%, correspondingly. Eventually, with fold-10, the SSODL-DFUDC approach attains average accubal, precn, and recal of 99.55%, 97.51%, and 97.55%, correspondingly. The TACC and VACC of the SSODL-DFUDC approach are investigated on DFU performance. The figure pointed out that the SSODL-DFUDC system has shown improved performance with improved values of TACC and VACC. It is perceptible that the SSODL-DFUDC system has reached maximal TACC outcomes. The classification results of the SSODL-DFUDC technique are inspected in the form of a confusion matrix. The results implied that the SSODL-DFUDC technique has successfully recognized the presence of normal and abnormal samples The TLS and VLS of the

Methods	Accuracy	Precision	Recall	F1-Score
SSODL-DFUDC	99.29	99.29	99.29	99.29
Inception-ResNet-v2	98.98	98.71	98.68	98.94
AlexNet	92.01	90.93	87.22	88.94
VGG16	97.87	92.21	90.18	90.67
DFUNet-KNN	95.63	93.75	92.39	93.00
DFUNet	96.97	94.17	92.11	92.75
DFUNet-SVM	96.23	95.17	92.86	94.09
GoogleNet	97.12	95.17	90.22	92.85
EfficientNet	98.89	98.64	98.54	99.11

Fig. 9. Comparative analysis of SSODL-DFUDC system with existing algorithms

SSODL-DFUDC method are tested on DFU performance in Fig. 5. The figure states that the SSODL-DFUDC technique has exposed improved performance with the lowest values of TLS and VLS. It is observable that the SSODL-DFUDC model has resulted in reduced VLS outcomes. An evident precision-recall study of the SSODL-DFUDC methodology in the test database is described in Fig. The figure implied that the SSODL-DFUDC system has led to superior values of precision-recall values in two classes. A detailed ROC study of the SSODL-DFUDC algorithm in the test database is exposed in Fig. The outcome stated the SSODL-DFUDC system has displayed its capability to classify two class labels. To illustrate the enhanced performance of the SSODLDFUDC technique, a widespread comparison study is made. The experimental values indicated that the AlexNet model reaches poor performance. At the same time, the DFUNet-KNN, DFUNet, and DFUNet-SVM models have attained slightly enhanced outcomes. Along with that, the VGG16 and GoogleNet models have obtained moderately improved performance. Although the EfficientNet model results in reasonable performance, the SSODL-DFUDC technique outperforms the existing ones with an increased accuy of 99.29%, precn of 99.29%, recal of 99.29%, and F1score of 99.29%. These results assured the improved performance of the SSODL-DFUDC technique in the classification process.

IV. CONCLUSION

In this article, we have developed a novel SSODL-DFUDC system to detect and classify DFU. The presented SSODLD-FUDC technique's goal lies in identifying and classifying

DFU. To accomplish this, the presented SSODL-DFUDC technique has applied the Inception-ResNet-v2 model for feature vector generation. In addition, the SSODL-DFUDC technique utilizes the SSO algorithm for hyperparameter tuning purposes. Moreover, the classification of DFU takes place using the SSAE model. The experimental results of the SSODL-DFUDC technique take place using the DFU dataset. In the future, the SSODL-DFUDC algorithm's performance can be improved by advanced DL classification models. In addition, weakly supervised learning techniques can be explored to reduce the dependency on precise pixel-level annotations. Instead of relying solely on expert-labeled ulcer regions, weakly supervised learning can utilize weak labels, such as image-level or bounding box annotations, making it more scalable and easier to collect data.

ACKNOWLEDGMENT

REFERENCES

[1] S. Wang, J. Wang, M. X. Zhu, and Q. Tan, "Machine learning for the prediction of minor amputation in university of Texas grade 3 diabetic foot ulcers," PLoS ONE, vol. 17, no. 12, Dec. 2022, Art. no. e0278445.

[2] M. Swerdlow, L. Shin, K. D'Huyvetter, W. J. Mack, and D. G. Armstrong, "Initial clinical experience with a simple, home system for early detection and monitoring of diabetic foot ulcers: The foot selfie," J. Diabetes Sci. Technol., vol. 17, no. 1, pp. 79–88, Jan. 2023.

[3] M. Goyal, N. D. Reeves, S. Rajbhandari, N. Ahmad, C. Wang, and M. H. Yap, "Recognition of ischaemia and infection in diabetic foot ulcers: Dataset and techniques," Comput. Biol. Med., vol. 117, Feb. 2020, Art. no. 103616.

[4] J. Yogapriya, V. Chandran, M. G. Sumithra, B. Elakkiya, A. S. Ebenezer, and C. S. G. Dhas, "Automated detection of infection in diabetic foot ulcer images using convolutional neural network," J. Healthcare Eng., vol. 2022, pp. 1–12, Apr. 2022

[5] K. S. Chan and Z. J. Lo, "Wound assessment, imaging and monitoring systems in diabetic foot ulcers: A systematic review,"Int. Wound J., vol. 17, no. 6, pp. 1909–1923, Dec. 2020.

[6] B. Cassidy, C. Kendrick, N. D. Reeves, J. M. Pappachan, C. O'Shea, D. G. Armstrong, and M. H. Yap, "Diabetic foot ulcer grand challenge 2021: Evaluation and summary," in Diabetic Foot Ulcers Grand Challenge. Cham, Switzerland: Springer, Sep. 2021, pp. 90–105.

[7] H. Pan, H. Peng, Y. Xing, L. Jiayang, X. Hualiang, T. Sukun, and F. Peng, "Breast tumour grading network based on adaptive fusion and microscopic imaging," Opto-Electron. Eng., vol. 50, no. 1, 2023, Art. no. 220158.

[8] Y. Wang, F. Luo, X. Yang, Q. Wang, Y. Sun, S. Tian, P. Feng, P. Huang, and H. Xiao, "The Swin-transformer network based on focal loss is used to identify images of pathological subtypes of lung adenocarcinoma with high similarity and class imbalance," J. Cancer Res. Clin. Oncol., vol. 149, no. 10, pp. 8581–8592, Sep. 2023.

[9] G. Du, Y. Li, P. Xie, X. Zhang, B. Deng, C. G. Wang, Y. Hu, M. Wang, W. Deng, D. Gu, X. Ma, and W. Deng, "The amputation and mortality of inpatients with diabetic foot ulceration in the COVID-19 pandemic and postpandemic era: A machine learning study," Int. Wound J., vol. 19, no. 6, pp. 1289–1297, Oct. 2022.